

## RESEARCH ARTICLE

# Key parameters in determining energy generated by CPV modules

Sarah Kurtz<sup>1\*</sup>, Matthew Muller<sup>1</sup>, Dirk Jordan<sup>1</sup>, Kanchan Ghosal<sup>2</sup>, Brent Fisher<sup>2</sup>, Pierre Verlinden<sup>3</sup>, Jun Hashimoto<sup>4</sup> and Daniel Riley<sup>5</sup>

<sup>1</sup> National Renewable Energy Laboratory, Golden, CO, USA

<sup>2</sup> Semprius, Durham, NC, USA

<sup>3</sup> State Key Laboratory of PV Science and Technology, Trina Solar, Changzhou, China

<sup>4</sup> Fukushima Renewable Energy Institute, National Institute of Advanced Industrial Science and Technology, Fukushima, Japan

<sup>5</sup> Photovoltaic and Distributed Systems Department, Sandia National Laboratories, Albuquerque, NM, USA

## ABSTRACT

We identify the key inputs and measurement data needed for accurate energy rating of concentrator photovoltaic (CPV) modules based on field observations of multiple CPV modules. Acceptance angle is shown to correlate with the observed module-level performance ratio (PR) for the modules studied. Using power ratings based on concentrator standard test conditions, PRs between 90% and 95% were observed during the summers with up to ~10% lower PRs during the winters. A module fabricated by Semprius showed 94%  $\pm$ 0.7% PR over almost 2 years with seasonal variation in PR of less than 1% showing how a module with relatively large acceptance angle may show very consistent average efficiency (calculated from the energy generated relative to the energy available), potentially simplifying energy ratings. The application of the results for translation of energy rating from one location to another is discussed, concluding that most of the translation differences may be correlated with temperature differences between sites with the largest variation happening when optical efficiency depends on temperature. Copyright © 2014 John Wiley & Sons, Ltd.

## KEYWORDS

energy yield; concentrator PV; performance ratio; acceptance angle; energy rating

### \*Correspondence

Sarah Kurtz, National Renewable Energy Laboratory, Golden, CO, USA.

E-mail: sarah.kurtz@nrel.gov

Received 29 April 2014; Revised 15 July 2014; Accepted 17 July 2014

## 1. INTRODUCTION

The efficiency of a photovoltaic (PV) system can vary with temperature, spectrum, and other factors complicating the estimation of electricity generated over a full year [1,2]. Flat-plate PV modules typically exhibit efficiency reduction with temperature by  $-0.25\%/^{\circ}\text{C}$  to  $-0.45\%/^{\circ}\text{C}$ , spectral effects of a few percent, and efficiency changes with irradiance that depend on the series and shunt resistances. These effects are well understood from the known dependencies of cell efficiency on operating conditions coupled with small effects associated with the stringing of the cells in the module. In addition, the angle of incidence of the light striking the outside of a flat-plate module affects the light that reaches the cells by a few percent. The angle of incidence effects are typically negligible within a  $45^{\circ}$  cone of normal incidence but become significant for

angles  $>65^{\circ}$  [1,2]. The angle of incidence effects could be classified as part of the optical efficiency of the module, where the optical efficiency reflects the incident light that reaches the cells.

The distinction between cell efficiency and optical efficiency is even more important for concentrator PV (CPV) because the efficiency of the concentrating optics varies much more strongly with angle of incidence and with other effects including soiling of the modules, inconsistent lens-cell alignment, inaccurate or inconsistent tracker pointing, variations in spectrum, change in focal length or focal position with thermal expansion, and scattering of the direct beam into the circumsolar component. Compared with flat-plate silicon, the efficiencies of multijunction cells operated under concentrated sunlight typically vary less with temperature but have a greater dependence on spectrum. Although the methodology for modeling the dependence

of CPV cell efficiency on operating conditions based on easily measured cell parameters has been defined and refined for a number of years [3–7], modeling the optical efficiency as a function of use conditions will require additional input parameters that have not been as well studied.

Ultimately, the owner of a PV system desires a method for understanding and predicting the energy yield of the PV system. Because of the variation of efficiency of a system with operating conditions and the variability of operating conditions for every site, energy rating procedures have been discussed for many years [8,9]. The International Electrotechnical Commission is developing an energy rating procedure for flat-plate modules [10–12] that characterizes the module efficiency as a function of irradiance and temperature then separately applies corrections for angle of incidence and spectrum.

Verlinden *et al.* proposed a simple energy rating procedure for CPV that uses a 6-month or year-long energy test as a basis then applies small corrections for translation of that result to other locations [5]. On the basis of an analysis of cell efficiency, Verlinden estimated the correction factors that need to be applied and concluded, for latitudes between 15° and 40°, very small corrections are needed for air mass. Spectral effects related to aerosol optical depth and precipitable water vapor (PWV) were estimated to be larger than the effect of cell temperature. This thorough analysis carefully quantified the effects related to cell efficiency but placed less emphasis on soiling and optical efficiency issues associated with the small acceptance angle of some CPV optics because of the difficulty of quantifying these effects.

Many studies have explored the expected efficiency of multijunction cells as a function of operating conditions and have sought to identify optimal designs for energy yield [3–7,13]. A key conclusion of these studies is that the instantaneous operating efficiency varies greatly (although this can be partially mitigated by luminescent coupling [14,15]), but the average efficiency (energy out divided by energy in) is much less sensitive to the cell design. Although careful correction must be made for variations in spectrum when ascribing a power rating for a CPV module, the requirements for ascribing an energy rating may have much less demanding requirements.

This paper complements many of the existing studies by studying measured data for more than a dozen modules and detailed data for two modules: one that shows a significant sensitivity to low temperatures and a design by Semprius that maintains its alignment over the temperature range studied here. The paper explores possible association between the measured acceptance angle of the modules with the measured performance throughout the year. The paper also discusses the possibility that a comparison of the performance during the summer and winter at a single location may be used as the basis for extrapolation of the data to other locations. The paper concludes with recommendations about the most important measurements that are needed to be included in an energy model that covers both the cell and optical efficiencies. The paper is limited

to module-level effects and concludes that system-level effects related to shading, soiling, and tracker operation may be larger than most module-level effects for CPV modules.

## 2. EXPERIMENTAL

Each CPV module was mounted on a two-axis tracker in Golden, Colorado, USA and the performance measured over months or years. The alignment was monitored with a four-quadrant tracking error monitor, and data with a tracking error of greater than 0.15° were discarded as a precaution. Every 5 min, the meteorological values and a full current–voltage (I–V) curve were recorded using a multitracer (Daystar Inc., Multitracer 5, RD=3200) if the direct normal irradiance (DNI) was greater than 100 W/m<sup>2</sup>. The multitracer was calibrated annually. Data were inspected for error codes or data out of range (e.g., negative data). Care was taken that if any part of the data record was missing or erroneous, the entire record was discarded. The modules were maintained at maximum power bias between scans. A pyrheliometer was used to quantify the DNI.

The use of performance ratio (PR) as a metric can vary because it depends on the power rating, which, if taken from the nameplate, may or may not match the power output of a specific module. To provide a consistent metric, the power ratings used in this study were derived for each module for concentrator standard test conditions (CSTC) using a filtered version of the data set [16]. Using a power rating derived in a consistent way for the module under test avoids the typical ambiguity of the PR caused by variation within a nameplate bin. Nevertheless, we emphasize that the PRs reported here are only at the module level. These data reflect the difference in temperature, irradiance, and spectrum experienced by the module over the course of the day but do not reflect stringing losses nor inverter losses that are included in the more common system-level PR [17]. Also, the uncertainty in the reported PR includes the uncertainties in the determination of CSTC as well as other measurement factors such as neglecting data during cloudy (<100 W/m<sup>2</sup> DNI) conditions and uncertainty in irradiance and power measurements.

The modules studied included a wide range of designs such as the domed lenses used in the Daido design, the very compact and small-cell design of Semprius, more conventional refractive designs, two reflective designs, and designs both with and without secondary optics. Module #1 was manufactured by Semprius [18]. This module has nominal dimensions of 635 mm × 475 mm and a thickness of 65 mm. The module backplane is an array of 660 printed three-junction microcells that are ~600 μm on each side. The primary optic is a silicone on glass plano-convex lens, and the secondary optic is a glass ball lens. The module has a geometric concentration of 1111X and has no external heat sinks or heat spreaders. The CSTC rating for this module was calculated to be 83.2 W based on the method described in [16]. Flash test data for this module were not available.

The two-axis tracker used in this study was designed to have high accuracy for the study of CPV module response as a function of changing conditions. The alignment is carefully controlled, but some data are missing because of other research activities (~95 days during the >700 days reporting period). In general, the modules and the pyrheliometer were cleaned once per week. Previous data collection showed that monthly cleaning of the modules was inadequate and that weekly cleaning gave data with reduced noise level.

The module alignment was confirmed relative to the tracker error monitor by scanning both the azimuth and elevation angles and plotting the module response as a function of the tracker error monitor signal on a clear day. We could find no evidence that tracker error affected the performance of any of the modules during the performance period; we could not distinguish the results before and after discarding the data for which either tracker error monitor reported  $>0.15^\circ$ .

Although PR is commonly used to characterize the AC output of a PV system relative to the module nameplate rating, it is convenient in this study to calculate the PR for the module only. Specifically, the sum of the maximum power (Pmp) data (from the I–V curves) is divided by the sum of the DNI (irradiance) data and normalized by the module CSTC power rating [16] divided by  $1000 \text{ W/m}^2$ . The CSTC ratings were derived from the on-sun performance data corrected for the difference between the operating cell temperature and  $25^\circ\text{C}$  [16].

### 3. MEASUREMENT AND ANALYSIS OF ACCEPTANCE ANGLE

We expect that understanding the acceptance angle will be a key part of understanding variations in the optical

efficiency of a CPV module. In the literature, sometimes, acceptance angles have been measured by plotting the short circuit current (Isc) and sometimes by plotting Pmp. To understand the difference between these and to demonstrate the general effect of internal misalignment within a module, a simplistic model is shown for a module with a single string of cells. Each lens-cell assembly is assumed to have exactly the same response to alignment, but each is misaligned from the rest by a small amount, as shown in Figure 1. Neglecting any shunting within each cell and assuming that each cell has a bypass diode that turns on at the short circuit condition, we estimate that the measured Isc of the module reflects the largest Isc in the string for a given alignment condition (see black, closed circle markers in Figure 1). Conversely, when currents are analyzed at the maximum power condition, the measured current is expected to nominally reflect the smallest Imp in the string (purple, open-circle markers in Figure 1). A full simulation would give slightly different results, but Figure 1 demonstrates why a larger acceptance angle is measured when Isc is documented compared with Imp or Pmp. Thus, the difference between Isc and Imp can reflect the internal misalignment of the cell. Previously, this relative difference has been referred to as the misalignment factor [19].

The effect of alignment was quantified from module I–V curves measured as a function of pointing error in the azimuth and elevation angles. For each I–V curve, the DNI and module temperature were measured. All values were linearly corrected for irradiance using the DNI data; the Pmax values were adjusted for module temperature variations assuming a temperature coefficient of  $-0.1\%/^\circ\text{C}$ . Figure 2 shows data for two modules with different designs. The left side of Figure 2 shows measurements for a module with good internal alignment. In this case, optimization of alignment can be accomplished by using either

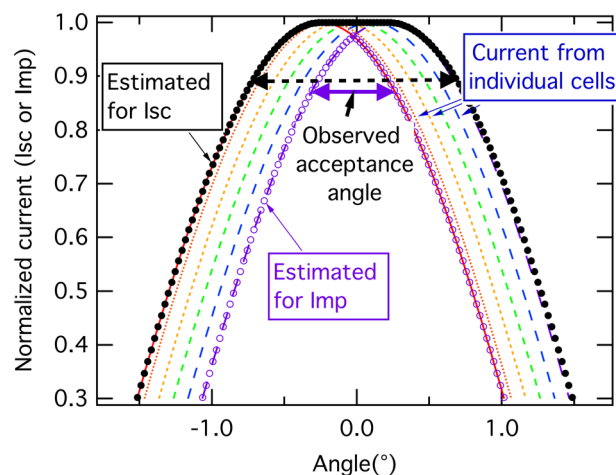


**Figure 1.** Simple model of current as a function of tracker error for a module with variable internal alignment. The dashed lines indicate the range of alignments assumed for the individual lens-cell assemblies. As described in the text, the black and purple markers indicate the nominal expected response as a function of pointing error when Isc or Imp is measured, respectively. Measurement of Isc will generally find a larger acceptance angle (dashed black horizontal arrows) compared with when Imp (or Pmp) is used (purple horizontal arrows) with the lens-cell acceptance angle falling in between.

Isc or Pmp. However, the right part of Figure 2 shows data for a module with variable internal alignment. Some I–V curves for this module showed steps in the I–V curve, implying turn on of bypass diodes, either because of variable cell quality or more likely (based on the measurements shown here) because of variable internal alignment. Alignment optimized for the Isc could be off for Pmp (which is what counts for electricity production) by as much as 0.2° in a case such as this. In either case, the acceptance angle of the module is best characterized by using the Pmp trace.

Data from scans similar to Figure 2 for about a dozen modules are summarized in Figure 3. Although acceptance angle is most commonly defined for a reduction to 90% in power, 98% was chosen for this documentation because energy output begins to be affected at this (98%) level and because one of the modules could not easily be measured to the 90% point (for scans beyond 0.8°, the DNI sensor becomes misaligned, complicating the data collection).

Within the uncertainty of the measurement, we expect that the acceptance angle measured from the Isc trace will be larger than that measured from the Pmp trace, as seen in Figure 3. The effect of the module design on the acceptance angle is shown by the different colors. For some of the manufacturers, the data reflect multiple generations of product, but the data are clustered, implying that the general design is more critical in determining the acceptance angle than small variations in design. Also, the clustering of the data by manufacturer gives confidence that the variation in measured acceptance angle with atmospheric conditions is a relatively small effect, because the measurements in Figure 3 were taken at different times during the year, although always on relatively clear days.

We seek to identify whether a small acceptance angle may reduce the energy when evaluating the energy generated by a module over the course of a year, especially at times when the air mass is large and the circumsolar (low

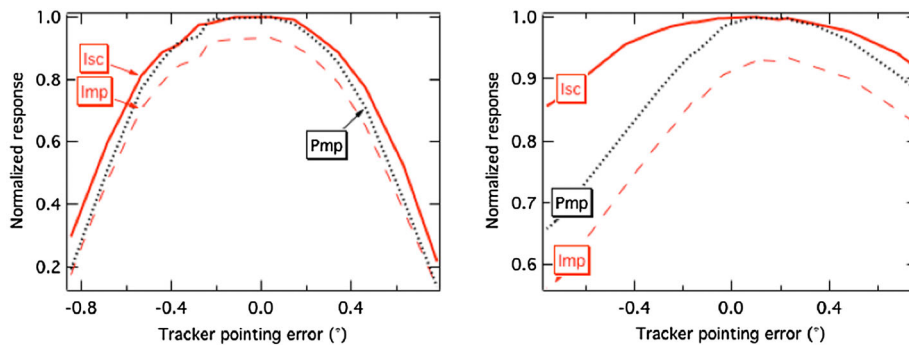


**Figure 2.** Data from a module with minimal (left) and with evident (right) internal misalignment. The Isc and Imp data were normalized to the maximum Isc value; the Pmp data were normalized to the maximum Pmp value.

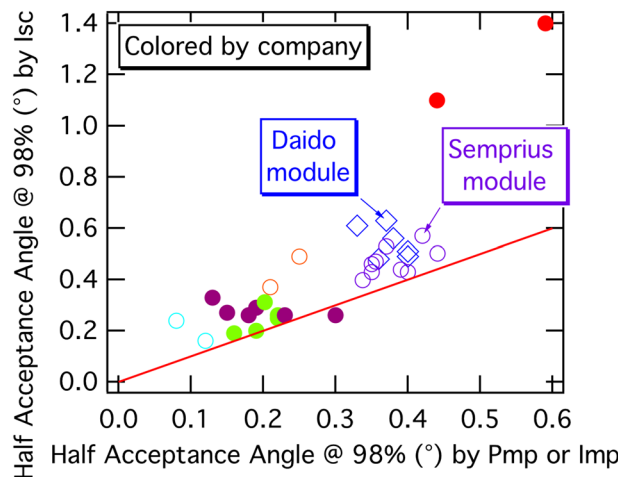


**Figure 3.** Comparison of measured acceptance angles at the 98% point using Isc and Pmp or Imp. Some of the data (for the Sempruis modules and one of the green solid circles) were measured at Sandia National Laboratories. The line indicates equality of the two measurements, implying excellent internal alignment of the module. The colors of the symbols reflect the company that manufactured the modules, sometimes reflecting multiple generations of product. In most cases, two points are presented per module, one each for the azimuthal and elevation scans, with more than a dozen modules represented. The points for half angle > 1° are estimated, because the DNI sensor response was not wide enough for the full scan.

angle) portion of the direct beam may be increased. In a full-size system, the tracker design is optimized by reducing the rigidity of the tracker to the point where the energy yield is affected, trading off the loss of energy with the reduced cost of the tracker. Although it is outside of the scope of this study to consider the system-level effects, we study here whether the carefully aligned performance is correlated with the acceptance angle of the module, recognizing that the effects may be greater if the tracker accuracy is not as carefully controlled. PR data for a set of modules are summarized as a function of acceptance angle at the 98% point in Figure 4 for summer and winter months. These five modules were chosen from more than a dozen modules represented in Figure 3 based on the availability of data, selecting months of data that had no anomalies. The five modules represent four different manufacturers, reflective and refractive optics, and designs with and without secondary optics.

Although there is substantial scatter in the data, there is a correlation between the acceptance angles and PR. During the summer, the effect is only ~3% for a relative increase of the 98% acceptance half angle from  $0.1^\circ$  to  $0.5^\circ$  (see line fit to summer data). However, during the winter, the effect may be as large as 10% over a similar range (see line fit to winter data). Explaining the variation of PR between summer and winter may provide most of the information needed to translate an energy rating obtained in one location to what would be expected in the second location; clearly, more work is needed before we will have a clear confidence in such a translation, but Figure 4 implies that seasonal variation may depend as much on optical efficiency variations (correlated with acceptance angle) as on cell efficiency variations.

The second possible explanation for the difference in PR between summer and winter could be related to the higher air mass during the winter and a difference in cell efficiency with the change in spectrum. The differences between the module designs in this respect were too small

to draw any clear conclusions about this aspect of module design from this data set. The averaging expected over the course of the year may minimize this effect for annualized PR [5].

#### 4. SEASONAL DEPENDENCE OF TEMPERATURE COEFFICIENTS AND SPECTRAL EFFECTS

Almost 2 years of data are summarized for two modules in Figure 5(a–b). We expect the instantaneous (power) efficiency to vary much more than the average (energy) efficiency over a longer time, so the daily, weekly, biweekly, and monthly PRs are plotted over the period as running averages. In the case of a day with  $< 0.1$  kWh/m<sup>2</sup> irradiance documented, the running average extended over a longer time period in order to identify the desired number of days with significant data. Cloudy days typically did not trigger data collection. Even though modeling of the instantaneous performance of these modules requires a detailed knowledge of the spectrum and other conditions, when the average performance is considered, the variation in performance is decidedly smaller and may be modeled with a much simpler model. The running averages were calculated from the integrated DNI and Pmp (from I–V curves) data rather than averaging the daily PR in order to maintain appropriate weighting of sunny days compared with partly cloudy days. Module #1 shows very little change in performance through the year, whereas module #2 shows a strong seasonal dependence with decreased performance during the winter.

Also shown in Figure 5 is the relationship between the 30-day rolling averages for the module performance and the DNI-weighted average ambient temperature. Although the PR for module #1 (Figure 5(c)) shows no obvious seasonal dependence, the normalized (to CSTC values) open-circuit voltage (Voc), fill factor (FF), and Isc to DNI ratio (labeled 'Isc') all show a seasonal dependence that correlates linearly with the temperature variation.

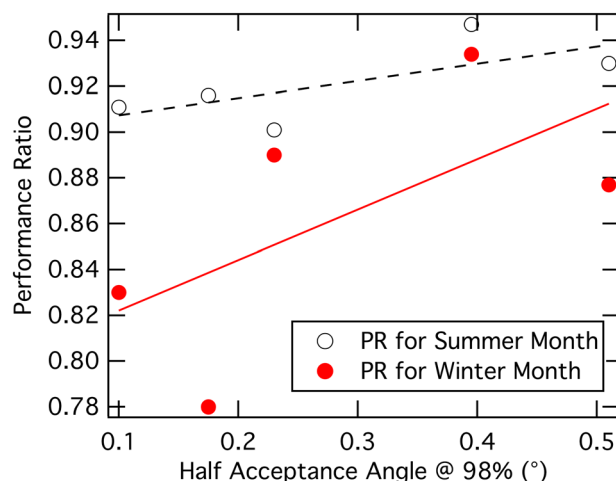


**Figure 4.** The performance ratio (PR) observed for a month of data as a function of acceptance angle for summer and winter months for five modules. The lines indicate least-square fits to each set of five data points.

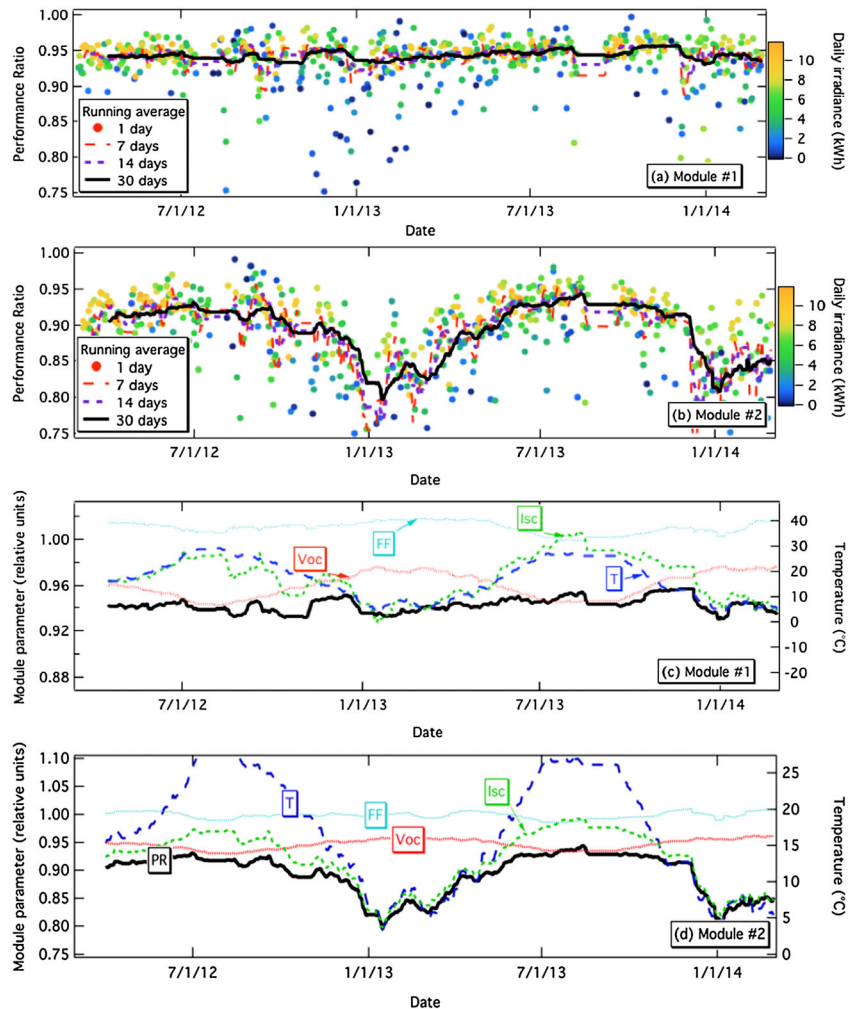


**Figure 5.** (a) and (b) Daily, weekly, biweekly, and monthly values of performance ratios for two modules. The daily data are colored according to the daily kWh of DNI as shown on the color scale. (c) and (d) Rolling 30-day averages of module parameters (normalized to CSTC rating) for modules #1 and #2 and their relationship to DNI-weighted ambient temperature. The relative scales have been adjusted for (c) and (d) to better show the relationships with the average temperature. The 30-day PR scans from (a) and (b) are duplicated in (c) and (d), respectively.

Other short-term variations were also observed; these appeared to be caused by extreme weather events such as sunny days with temperatures  $<0^{\circ}\text{C}$  or turbidity (aerosol optical depth at 500 nm) values  $>0.5$ . These types of events only occurred about once per year in this data set, providing insufficient data to fully assess the expected impact or the exact limits for module #1 and are likely to be of little consequence in most high DNI areas for which CPV is best suited. Nevertheless, the observation that these extreme events affect the performance highlights the importance of exploring the effects of extreme conditions when extrapolating an energy rating to a new location for which those conditions may be more common. The very small dependence of response on temperature for module #1 can be seen on the left side of Figure 6.

For module #2, Figure 5(d) compares the time variation of the PR with the variation in the DNI-weighted average

ambient temperature. During warm weather, the PR of module #2 is fairly constant with minimal evidence of seasonal variations, but when the ambient temperature during operation drops below  $\sim 12^{\circ}\text{C}$ , the PR also decreases. The cause of this can be seen in Figure 6 (right side), which shows the normalized  $I_{sc}$  as a function of the ambient temperature. Above  $\sim 15^{\circ}\text{C}$ , the  $I_{sc}$  of module #2 shows little dependence on the ambient temperature. Below  $\sim 15^{\circ}\text{C}$ ,  $I_{sc}$  decreases  $\sim 1\%/^{\circ}\text{C}$ , explaining the decrease in performance seen in Figure 5(d) for the lower temperatures.

## 5. DISCUSSION

Concentrator photovoltaic modules are mostly immune to the seasonal variations associated with angle of incidence effects on the optical efficiency of most flat-plate systems

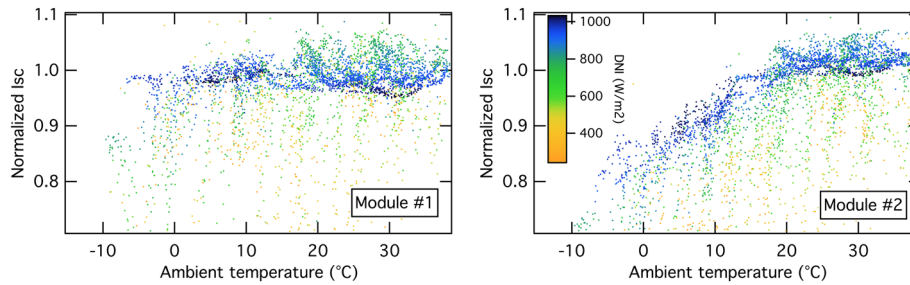


**Figure 6.** Short circuit current ( $I_{sc}$ ) as a function of ambient temperature for (left) modules #1 and (right) #2. The  $I_{sc}$  is normalized by the measured DNI and the module  $I_{sc}$  rating. The data were taken from June and December of 2012 and are colored by DNI as shown in the color scale.

because of two-axis tracking. Similarly, the lack of response to diffuse light implies a more consistent set of conditions for CPV (cloudy days do not appear in the analysis, whereas studies of flat-plate systems often need to treat these separately and need to cover a wider range of climates). However, these simplifying features of CPV are overshadowed by the complex factors that determine the optical efficiency including multiple aspects of alignment (at the cell, module, and tracker levels), greater sensitivity to soiling, wind stow and wind flutter. This study used a tracker with careful control of the alignment, so system-level issues such as pedestal-to-pedestal shading and tracker misalignment were removed. Also, it was found that monthly cleaning left substantial noise associated with soiling, so the modules were cleaned weekly for the two modules studied carefully here, again neglecting an issue that may dominate system-level performance.

Although the data in Figure 4 are too sparse to have strong confidence, they imply that a reduction in the measured half acceptance angle (at 98%) from  $0.5^\circ$  to  $0.1^\circ$  may decrease the PR by  $\sim 3\%$  in summer and  $10\%$  in winter. A key value of a year-long energy test is that it quantifies the energy losses associated with small acceptance angle without requiring detailed estimates of scattering of the direct beam into the circumsolar part of the beam and the associated modeling of light capture of the circumsolar portion of the direct beam. However, even though the year-long test quantifies the losses for one location, the translation of these losses to other locations may be more difficult.

Module #1 (the Semprius module) exhibited an average PR of 94.2% with variation of  $\pm 0.7\%$  calculated from the 30-day average PR over almost 2 years time. Factors identified as being important in achieving this high PR included a relatively large  $\sim 0.4^\circ$  half acceptance angle at 98%, consistent alignment even at  $< 12^\circ\text{C}$ , and optimization for an air mass of  $\sim 2.5$ , which is well matched for this location. Module #2 exhibited a lower PR, especially during winter months when there is evidence that lower temperatures reduced the optical efficiency. On the basis of these observations, we suggest that the 30-day average PRs at the module level for CPV modules may be expected to fall in the range of 90–95% depending on the acceptance angle and spectral design (air mass for which the cell efficiency is optimized) as long as the capability of the design falls within the temperature range of the sites being considered.

A year-long energy test provides an assessment of the effects of acceptance angle, spectral (air mass) optimization, and problems with extreme temperatures (for the measurement location). On the basis of this limited data set, for modules with acceptance angles large enough not to be affected by variations of the circumsolar component of the direct beam, translation of the annual PR to the second location may be successful within  $\sim 2\%$  using a simple correction for temperature. This correction requires two parts: the first is an assessment of the effects of extreme temperatures on the optical efficiency. Essentially, all optical designs will decrease in efficiency if the temperature is changed enough because of differences in thermal expansion coefficient of the multiple materials. Module manufacturers should test the module performance at extreme temperatures to identify the range beyond which the module efficiency will be anomalously reduced. For module #2 studied here, the  $1\%/^\circ\text{C}$  coefficient for the optical efficiency observed below  $\sim 15^\circ\text{C}$  causes a much larger variation in efficiency than the cell efficiency temperature coefficient, (approximately  $-0.1\%/^\circ\text{C}$ ). The second part of the temperature correction is more difficult, but we expect that the needed correction is small enough that it may be neglected or crudely approximated. As confirmed here for module #1 and as summarized in Table I, a difference of  $\sim 20^\circ\text{C}$  in the average temperature found during the summer and the winter translates to  $\sim 3\%$  difference in Voc. This is very consistent with the measured Voc temperature coefficient of  $-0.147\% \pm 0.02\%/^\circ\text{C}$  for module #1 (measured on module #1). The variation in average FF is  $\sim 2\%$  from summer to winter.  $I_{sc}$  varies  $\sim 5\%$  between summer and winter but also varies  $\sim 2\%$  randomly. The variation in  $I_{sc}$  is expected to depend on the interrelated effects of air mass, PWV, and atmospheric turbidity. The energy-weighted or 50th percentile air mass is directly related to the latitude of deployment. Our analysis agrees with the study of Verlinden *et al.*, who concluded that for latitudes between  $15^\circ$  and  $40^\circ$ , no correction is needed [5]. The precipitable water vapor is highly dependent on the temperature of the atmosphere, showing a seasonal dependence that correlates with the average temperature and may, therefore, be successfully handled by a correction factor associated with temperature. The turbidity is more difficult to correct for because accurate measurements of

**Table 1.** Translation requirements expected for module performance based on this study. If a statement pertains only to module #2 (that shows temperature-sensitive alignment), it is noted. Otherwise, the statements reflect approximate data from both modules and are expected to be relevant to the majority of CPV modules that use GaInP/GaAs/Ge cells.

| Factor   | Size of variation observed  | Suggested correction method  |
|--|---|--|
| Decrease in optical efficiency because of extreme temperatures | 10% reduction in PR was observed during winter months for module #2; smaller decreases during the winter were seen for other modules.   | Test the module at extreme temperatures; many modules require no correction, but the temperature range should be characterized for all modules.  |
| Voc change with temperature                                    | 3% between summer and winter for 20–25°C temperature change, comparable with the difference between Phoenix, AZ, and Caribou, Maine for which annual average maximum $T$ is 30 and 9°C, respectively [21].  | Either assume that the Isc variations will complement the Voc variations or use average temperature and Voc temperature coefficient ( $-0.15\%/^{\circ}\text{C}$ )                                   |
| FF change with temperature and spectrum                        | 2% between summer and winter for 20–25°C temperature change, comparable with the difference between Phoenix, AZ and Caribou, Maine for which annual average maximum $T$ is 30 and 9°C, respectively [21].   | Either assume that the Isc variations will complement the FF variations or use average temperature and FF temperature coefficient ( $-0.05\%/^{\circ}\text{C}$ )                                     |
| Isc change with optical efficiency, temperature, and spectrum  | 5% between summer and winter. <sup>a</sup> The AM difference between summer and winter corresponds to a latitude variation from $\sim 20^{\circ}$ to $\sim 60^{\circ}$ [3]. Average precipitable water vapor varied from 0.5 (winter) to 2 (summer) cm. | First, focus on estimating the effects of soiling then consider whether to model water vapor, turbidity, and AM effects coupled with acceptance angle analysis or accept the uncertainty of a few %. |

CPV, concentrator photovoltaic; PR, performance ratio; Voc, open-circuit voltage; Isc, short circuit current; FF, fill factor; AM, air mass.

<sup>a</sup>Monthly DNI-weighted air mass varied from 1.7 to 3.5 and average water vapor from 0.5 to 2 cm.

turbidity are uncommon. However, the effects of high turbidity are increased by both higher air mass and higher water vapor, because the particles in the atmosphere tend to swell slightly in moist environments, causing greater scattering. So, it is possible that the first approximation corrections for turbidity may be lumped into a correction for temperature. Also, the primary effect of high turbidity is a reduced DNI, which is accounted for separately. Skies in Colorado tend to be clearer than in many other locations, so the need for corrections for turbidity should be further explored.

The measured efficiency relative to DNI measured by a pyrheliometer is more dependent on PWV values between 0.5 and 1 cm; above PWV of 1 cm, the water bands in the infrared are mostly saturated and added moisture has little effect on the transmitted light [20]. The sensitivity to PWV may be mostly removed if the irradiance is measured with matched reference cells. Similarly, the concern with variable circumsolar radiation may be reduced or eliminated by using irradiance sensors that have optical response mimicking that of the module under test, as suggested by Verlinden *et al.* [5]. Although the use of matched reference cells mounted in a fixture with matched optical efficiency would improve the accuracy of an energy rating, the measured irradiance would differ from historical weather data, making it challenging for an investor to assess the expected energy yield at a location that has not yet been characterized with the matched reference cells.

Although this study focused only on module data, it is useful to consider how these results may be applied at the system level. We noted that monthly cleaning instead of weekly cleaning resulted in noisier data, highlighting the importance of soiling even in the relatively clean environment found in our paved array field. Thus, we expect that translation of system-level data from one location to another may require correction for variable soiling losses as well as changes in shading because of changing system size or geometry, wind stow, and tracker alignment associated with wind variations. The detailed analysis of Isc translation is expected to include the changing effects of spectrum associated with air mass, turbidity, and water vapor. However, the data presented here would imply that it is more important to consider the effects of changes of optical efficiency with temperature and the interplay between acceptance angle and changing conditions. Specifically, modules with small acceptance angles may show a reduced apparent optical efficiency for higher air masses because of the additional small-angle scattering, increasing the need to correct for changing latitude more than expected by modeling the cell response alone. To achieve an accuracy of 1% prediction in energy for a new plant, all spectral effects must be carefully corrected for. But this study suggests that uncertainties associated with soiling (reported to be as high as 26% after no rain for 4 months for CPV [21]) may be much larger than the various spectral effects

(here found to be typically <5%), reducing the pressure to make careful spectral measurements and models.

## 6. CONCLUSION

Five modules exhibited PRs for summer performance between 90% and 95%; the lower PRs were correlated with smaller acceptance angles. The decrease in PR for smaller acceptance angles appeared to be greater during the winter, underscoring the importance of characterizing (i) the temperature range over which the optical design retains efficiency; (ii) the acceptance angle; and (iii) the reduction in performance with higher air mass, especially for modules with small acceptance angles.

In addition, two CPV modules were characterized during almost 2 years. During this time, studying daily, weekly, and monthly PRs, one of the modules showed no seasonal variation in performance that could be differentiated from random noise. The second module showed a seasonal effect of ~10%, highlighting the importance of understanding the optical efficiency at extreme temperatures.

The small seasonal variations that are documented here provide optimism that the results of an energy test in one location may be translated to the second location with minimal adjustments, especially for modules with large acceptance angles and optical efficiency that is independent of the temperature.

Variable operating conditions can cause reduced PRs, but here, we document an average PR of 94% over almost 2 years of operation for the Semprius module, which is comparable with the annual PR observed for flat-plate modules in this location, underscoring how small the energy losses associated with variable spectrum for multijunction cells are.

## ACKNOWLEDGEMENTS

The authors wish to thank J. Rodriguez for his technical assistance with the tracker and data collection and T. Silverman, M. Deceglie, and J. Wohlgemuth for their useful comments on the manuscript. This work was completed under contract no. DE-AC36-99GO10337 with the US Department of Energy.

## REFERENCES

- De Soto W, Klein SA, Beckman WA. Improvement and validation of a model for photovoltaic array performance. *Solar Energy* 2006; **80**(1): 78–88. DOI: 10.1016/j.solener.2005.06.010
- King DL, Kratochvil JA, Boyson WE. Photovoltaic array performance model (United States Department of Energy, 2004.
- Faine P, Kurtz SR, Riordan C, Olson J. The influence of spectral solar irradiance variations on the performance of selected single-junction and multijunction solar cells. *Solar Cells* 1991; **31**(3): 259–278.
- Kurtz SR, Olson JM, Faine P. The difference between standard and average efficiencies of multijunction compared with single-junction concentrator cells. *Solar Cells* 1991; **30**(1–4): 501–513. DOI: 10.1016/0379-6787(91)90081-Y
- Verlinden PJ, Lasich JB. Energy rating of concentrator PV systems using multi-junction III-V solar cells. Photovoltaic Specialists Conference, 2008. PVSC '08. 33rd IEEE, 2008; p. 1–6. DOI: 10.1109/pvsc.2008.4922912
- Rodrigo P, Fernandez EF, Almonacid F, Perez-Higueras PJ. Models for the electrical characterization of high concentration photovoltaic cells and modules: a review. *Renewable and Sustainable Energy Reviews* 2013; **26**: 752–760. DOI: 10.1016/j.rser.2013.06.019
- Steiner M, Siefert G, Hornung T, Peharz G, Bett AW. Yieldopt, a model to predict the power output and energy yield for concentrating photovoltaic modules. *Progress in Photovoltaics: Research and Applications* 2014. DOI: 10.1002/ppp.2458
- Kroposki B, Emery K, Myers D, Mrig L. A comparison of photovoltaic module performance evaluation methodologies for energy ratings, Photovoltaic Energy Conversion, 1994., Conference Record of the Twenty Fourth. IEEE Photovoltaic Specialists Conference-1994, 1994 IEEE First World Conference on, 1994 (IEEE); p. 858–862.
- Kenny R, Friesen G, Chianese D, Bernasconi A, Dunlop E. Energy rating of PV modules: comparison of methods and approach, Photovoltaic Energy Conversion, 2003. Proceedings of 3rd World Conference on, 2003 (IEEE); p. 2015–2018.
- IEC 61853-3 - Draft H. Photovoltaic (PV) Module Performance Testing and Energy Rating - Part 3: Energy Rating of PV Modules, IEC Central Office: Geneva, Switzerland, 2012.
- IEC 61853-2 - CDV. Photovoltaic (PV) module performance testing and energy rating - part 2: spectral response, incidence angle and module operating temperature measurements, IEC Central Office: Geneva, Switzerland, 2012.
- IEC 61853-1. Photovoltaic (PV) module performance testing and energy rating - part 1: irradiance and temperature performance measurements and power rating, IEC Central Office: Geneva, Switzerland, 2011.
- Araki K, Yamaguchi M, Kondo M, Uozumi H. Which is the best number of junctions for solar cells under ever-changing terrestrial spectrum?," 3rd World Conference on PV Energy Conversion, 2003; p. 307.
- Brown AS, Green MA. Radiative coupling as a means to reduce spectral mismatch in monolithic tandem

- solar cell stacks-theoretical considerations, 29th IEEE Photovoltaic Specialists Conference, New Orleans, Louisiana, 2002 (IEEE, New York); p. 868–871.
15. Friedman DJ, Geisz JF, Steiner MA. Analysis of multijunction solar cell current-voltage characteristics in the presence of luminescent coupling. *Photovoltaics, IEEE Journal of* 2013; **3**(4): 1429–1436. DOI: 10.1109/jphotov.2013.2275189
  16. Muller M, Kurtz S, Steiner M, Siefer G. Translating outdoor CPV I-V measurements to a CSTC power rating and the associated uncertainty, to be published, 2014.
  17. IEC 61724. Photovoltaic system performance monitoring - guidelines for measurement, data exchange and analysis, IEC Central Office: Geneva, Switzerland, 1998.
  18. Ghosal K, Lilly D, Gabriel J, Whitehead M, Seel S, Fisher B, Wilson J, Burroughs S. Semprius field results and progress in system development. *Photovoltaics, IEEE Journal of* 2014; **4**(2): 703–708. DOI: 10.1109/jphotov.2013.2288026
  19. Peharz G, Ferrer Rodriguez JP, Siefer G, Bett AW. A method for using CPV modules as temperature sensors and its application to rating procedures. *Solar Energy Materials and Solar Cells* 2011; **95**(10): 2734–2744.
  20. Muller M, Marion B, Kurtz S, Rodriguez J. An investigation into spectral parameters as they impact CPV module performance. *AIP Conference Proceedings* 2010; **1277**(1): 307–311. DOI: 10.1063/1.3509218
  21. Vivar M, Herrero R, Moreton R, Martinez-Moreno F, Sala G. Effect of soiling on PV concentrators: comparison with flat modules, Photovoltaic Specialists Conference, 2008. PVSC '08. 33rd IEEE, 2008; p.1–4. DOI: 10.1109/pvsc.2008.4922915